

ANALYTICAL TECHNIQUE TO EVALUATE THE ASYMPTOTIC PART OF THE IMPEDANCE MATRIX OF MICROSTRIP DIPOLE ON A UNIAXIAL SUBSTRATE

K. Li, S.-O. Park, H. Lee, and J. Ma

School of Engineering
Information and Communications University
58-4 Hwaam-dong, Yusung-Gu, Taejon, 305-732, South Korea

B.-C. Kim and H.-D. Choi

Electronics Telecommunications Research Institute (ETRI)
161 Jajong-Dong, Yusong-Gu, Taejon, 305-350, South Korea

Abstract—The integral transform method with the asymptotic extraction technique is formulated to evaluate a Sommerfeld type integral for the analysis microstrip dipole on a uniaxial substrate. The infinite double integral of the asymptotic part of the impedance matrix with triangular subdomain basis function with edge condition can be reduced to a finite one-dimensional integral. This finite one-dimensional integral can be easily evaluated numerically after the singular part of the integral is treated analytically. It is demonstrated the efficiency and accuracy of the proposed method to evaluate the asymptotic part of impedance matrix.

1 Introduction

2 Theory

3 Integral Transform Technique

4 Evaluation of the Integral I_{mn}^c

5 Computations and Comparisons

6 Conclusion

References

1. INTRODUCTION

The Moment Method (MoM) has been successful for the analysis of usual antennas on anisotropic substrates. Good results can be given for the analysis of microstrip dipoles and circuits based on MoM, but suffer from the necessity of extremely accurate evaluations of the impedance matrix elements. For the accurate and efficient computation of these impedance matrix elements on an isotropic dielectric slab, the analytical technique for calculating the asymptotic part of the impedance matrix element in the spectral domain was presented in order to improve the computational efficiency of these matrix elements [7].

In this paper, based on the extract Green's function for the uniaxial substrate [9], the integral transform method with the asymptotic extraction technique is formulated to evaluate a Sommerfeld type integral with the extension of work in [7]. For the electrically narrow microstrip line structures on a uniaxial substrate, the infinite double integral of the asymptotic part of the impedance matrix element can be transformed into a finite one-dimensional integral by using the asymptotic Green's function and the triangular basis function with edge condition. This finite one-dimensional integral can be easily evaluated. Similarly, these results can be applied to solve microstrip dipole problems on a uniaxial substrate.

2. THEORY

In Fig. 1, the geometry of an infinitesimal \hat{x} directed unit current element on a uniaxial dielectric substrate is shown, where the unit infinitesimal current source is located at (x_0, y_0, d) . The dielectric can be characterized by a permittivity tensor of the form

$$\bar{\epsilon} = \epsilon_0 \begin{bmatrix} \epsilon_x & 0 & 0 \\ 0 & \epsilon_x & 0 \\ 0 & 0 & \epsilon_z \end{bmatrix}. \quad (1)$$

The space above the substrate ($z > d$) is assumed to be occupied by an isotropic and homogeneous medium ϵ_0 and μ_0 denoting the permittivity and permeability values, respectively.

In planar structures for the uniaxially anisotropic case, such as microstrip dipoles and discontinuities in microstrip lines, a typical moment method impedance matrix element in the spectral domain may be expressed in the form [9]

$$\bar{\bar{Z}}_{mn} = -\frac{1}{4\pi^2} \int_{-\infty}^{\infty} \int_{-\infty}^{\infty} \vec{J}_m(k_x, k_y) \bar{\bar{G}}(k_x, k_y) \vec{J}_n^*(k_x, k_y) dk_x dk_y \quad (2)$$

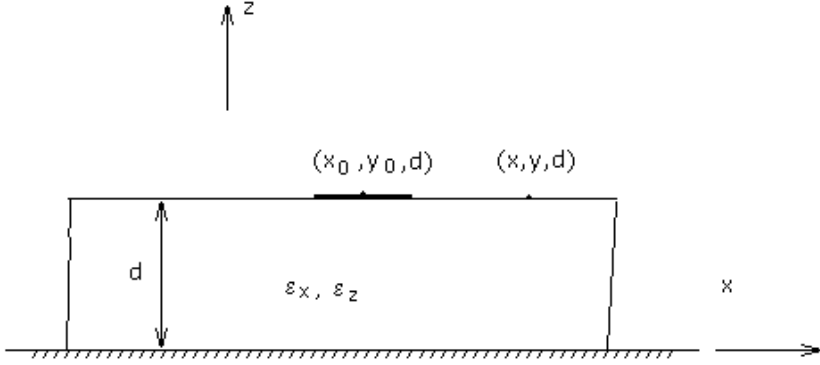


Figure 1. Geometry of an infinitesimal \hat{x} -directed unit current element on a uniaxial dielectric substrate.

where \tilde{J}_m is the Fourier transform of the basis function and $\overline{\overline{G}}$ is the dyadic Green's function in the spectral domain for the structure of interest.

In this paper, we should define the dyadic Green's function due to an infinitesimal current source on a uniaxial dielectric substrate. Similar to that of [7], only the Z_{mn}^{xx} matrix of (2) involving the Green's function \tilde{G}_{xx} needs to be evaluated for the very thin width of the strip. The Green's function \tilde{G}_{xx} is taken the form of [9]

$$\tilde{G}_{xx}(k_x, k_y) = -\frac{jZ_0}{k_0} \left[\frac{k_x^2 k_2 k_b \tan(k_b d)}{\beta^2 T_m} + \frac{k_0^2 k_y^2 \tan(k_a d)}{\beta^2 T_e} \right] \quad (3)$$

where

$$\begin{aligned} T_e &= k_a + jk_2 \tan(k_a d) \\ T_m &= \epsilon_x k_2 + jk_b \sin(k_b d) \\ k_a^2 &= \epsilon_x k_0^2 - \beta^2, \quad \text{Im}\{k_a\} < 0 \\ k_b^2 &= \epsilon_x k_0^2 - \epsilon_x \beta^2 / \epsilon_z, \quad \text{Im}\{k_b\} < 0 \\ k_2^2 &= k_0^2 - \beta^2, \quad \text{Im}\{k_2\} < 0 \\ \beta^2 &= k_x^2 + k_y^2, \\ k_0 &= \omega \sqrt{\mu_0 \epsilon_0} = 2\pi / \lambda_0, \quad \omega = 2\pi f \\ Z_0 &= \sqrt{\frac{\mu_0}{\epsilon_0}} \end{aligned} \quad (4)$$

where f and λ_0 are the frequency and the free space wavelength, respectively.

Employing the asymptotic extraction technique to improve the computation efficiency, the integral of (2) can be written as

$$\begin{aligned} Z_{mn}^{xx} = & -\frac{1}{4\pi^2} \int_{-\infty}^{\infty} \int_{-\infty}^{\infty} \tilde{J}_{xm}(k_x, k_y) [\tilde{G}_{xx}(k_x, k_y) - \tilde{G}_{xx}^{\infty}(k_x, k_y)] \\ & \cdot \tilde{J}_{xn}^*(k_x, k_y) dk_x dk_y \\ & - \frac{1}{4\pi^2} \int_{-\infty}^{\infty} \int_{-\infty}^{\infty} \tilde{J}_{xm}(k_x, k_y) \tilde{G}_{xx}^{\infty}(k_x, k_y) \tilde{J}_{xn}^*(k_x, k_y) dk_x dk_y \end{aligned} \quad (5)$$

The first integral in (5) converges more rapidly to zero than the double integral of (2). The integrand of the second integral exhibits slowly convergent and highly oscillatory behavior, which leads to difficulties when using a direction numerical evaluation. Therefore, in this paper, emphasis is placed on finding an efficient solution of the asymptotic part of impedance matrix elements [the second integral in (5)] by using the integral transform technique. To investigate the efficient evaluation of the second integral in (5), we investigate the asymptotic behavior of the Green's function for a uniaxial substrate, for large k_x and k_y , which can be derived easily

$$\tilde{G}_{xx}^{\infty} \approx -j \frac{Z_0}{k_0} \left[\frac{k_0^2}{2\beta} - \frac{k_x^2}{\beta(1 + \sqrt{\epsilon_x \epsilon_z})} + \frac{k_x^2 k_0^2 (\sqrt{\epsilon_x} - \sqrt{\epsilon_z})^2}{4\beta(1 + \sqrt{\epsilon_x \epsilon_z})\beta^2} \right]. \quad (6)$$

In the next step, the triangular subdomain basis function with edge condition is used to describe the anticipated currents on the electrically narrow microstrip lines. The longitudinal current densities of the triangular basis function with edge condition are denoted by $J_{xm}(x, y)$, where $J_{xm}(x, y)$ is defined as

$$J_{xm}(x, y) = \frac{1 - \frac{|x - x_m|}{L}}{\sqrt{1 - \left(\frac{2y}{W}\right)^2}}, \quad \left| \frac{2y}{W} \right| < 1, \quad \left| \frac{x - x_m}{L} \right| < 1 \quad (7)$$

where W is the width of the strip, and L is the half-length of the basis function.

The Fourier transforms of these functions can be written as

$$\begin{aligned} \tilde{J}_{xm}(k_x, k_y) &= \int_{-\infty}^{\infty} \int_{-\infty}^{\infty} J_{xm}(x, y) e^{-j(k_x x + k_y y)} dx dy \\ &= 2\pi \frac{W}{L} \frac{\sin^2\left(k_x \frac{L}{2}\right)}{k_x^2} e^{-jx_m k_x} \cdot J_0\left(k_y \frac{W}{2}\right) \end{aligned} \quad (8)$$

where J_0 is the zero order Bessel function of the first kind.

Substituting (8) into the second integral of (5), the asymptotic part of impedance matrix can be expressed as

$$Z_{mn}^{Asy} = -j \frac{1}{\pi^2} \frac{Z_0}{k_0} \left(2\pi \frac{W}{L} \right)^2 \cdot \left\{ -\frac{k_0^2}{2} I_{mn}^a + \frac{1}{(1 + \sqrt{\epsilon_x \epsilon_z})} I_{mn}^b - \frac{k_0^2 (\sqrt{\epsilon_x} - \sqrt{\epsilon_z})}{4(1 + \sqrt{\epsilon_x \epsilon_z})} I_{mn}^c \right\} \quad (9)$$

with

$$I_{mn}^a = \int_0^\infty \int_0^\infty \frac{\cos(x_s k_x)}{\sqrt{k_x^2 + k_y^2}} \frac{\sin^4\left(k_x \frac{L}{2}\right)}{k_x^4} \left[J_0\left(k_y \frac{W}{2}\right) \right]^2 dk_x dk_y \quad (10)$$

$$I_{mn}^b = \int_0^\infty \int_0^\infty \frac{\cos(x_s k_x)}{\sqrt{k_x^2 + k_y^2}} \frac{\sin^4\left(k_x \frac{L}{2}\right)}{k_x^2} \left[J_0\left(k_y \frac{W}{2}\right) \right]^2 dk_x dk_y \quad (11)$$

$$I_{mn}^c = \int_0^\infty \int_0^\infty \frac{\cos(x_s k_x)}{(k_x^2 + k_y^2)^{3/2}} \frac{\sin^4\left(k_x \frac{L}{2}\right)}{k_x^2} \left[J_0\left(k_y \frac{W}{2}\right) \right]^2 dk_x dk_y \quad (12)$$

where x_s is defined as $|x_m - x_n|$.

The analytical solutions to (10) and (12) have an integrable singularity at $\beta = 0$. The analytical solutions to (10) and (11) have been addressed by Park and Balanis [7]. The analytical solution to (12) is the subject in this paper.

3. INTEGRAL TRANSFORM TECHNIQUE

The integrand in (12) is not separable in terms of k_x and k_y due to the $1/(k_x^2 + k_y^2)^{3/2}$ term, which prevents it from being reduced to the product of one-dimensional integral. By using the infinite integral formula 6.691 of [16] in terms of χ

$$\frac{1}{\pi} \int_{-\infty}^{\infty} K_0(k_y |\chi|) \sin(k_x \chi) \chi d\chi = \frac{k_x}{(k_x^2 + k_y^2)^{3/2}}, \text{ if } k_x, k_y \text{ are real, } k_y > 0 \quad (13)$$

where K_0 is the modified Bessel function of the first kind.

I_{mn}^c can be expressed as

$$I_{mn}^c = \frac{1}{\pi} \int_{-\infty}^{\infty} \left\{ \int_0^{\infty} K_0(k_y|\chi|) \left[J_0\left(k_y \frac{W}{2}\right) \right]^2 dk_y \right. \\ \left. \times \int_0^{\infty} \sin(k_x\chi) \cos(k_x x_s) \frac{\sin^4\left(k_x \frac{L}{3}\right)}{k_x^3} dk_x \right\} \chi d\chi. \quad (14)$$

The three-fold integrations of (14) can be converted into only one-dimensional integrals in terms of χ if the separate double integrals with respect to k_x and k_y in (14) can be solved analytically.

By using formula 6.513.2 of [16], the first integral in (14) with respect to k_y can be expressed explicitly as

$$\int_0^{\infty} K_0(k_y|\chi|) \left[J_0\left(k_y \frac{W}{2}\right) \right]^2 dk_y \\ = \frac{1}{2|\chi|} \left[\Gamma\left(\frac{1}{2}\right) \right]^2 \left[P_{-\frac{1}{2}} \left(\sqrt{1 + \left(\frac{W}{|\chi|}\right)^2} \right) \right]^2 \quad (15)$$

where $P_{-\frac{1}{2}}$ is the spherical Legendre function of the first kind.

For convenience of notation, the function that appears in (15) is defined as

$$A(|\chi|) = \frac{1}{|\chi|} \left[P_{-\frac{1}{2}} \left(\sqrt{1 + \left(\frac{W}{|\chi|}\right)^2} \right) \right]^2 \quad (16)$$

After using formula 3.828.15 of [16], we introduce the following formula to evaluate the integration of the second integral in (14) with respect to k_x as follows;

$$\tau(x) = \int_0^{\infty} \frac{\sin^3\left(k_x \frac{L}{2}\right)}{k_x^3} \cos(k_x x) dk_x \\ = \begin{cases} \frac{\pi}{8} \left(\frac{3L^2}{4} - |x|^2 \right) & , \quad |x| < \frac{L}{2} \\ \frac{\pi}{16} \left(\frac{3L}{2} - |x| \right)^2 & , \quad \frac{L}{2} \leq |x| < \frac{3L}{2} \\ 0 & , \quad |x| \geq \frac{3L}{2} \end{cases} \quad (17)$$

Substituting (17) into (14), the second integral in (14) with respect to k_x is represented by

$$\begin{aligned} \Im_c(\chi) &= \int_0^\infty \frac{\sin^4\left(k_x \frac{L}{2}\right)}{k_x^3} \sin(k_x \chi) \cos(k_x x_s) dk_x \\ &= \frac{1}{4} \left[\tau\left(\chi + x_s - \frac{L}{2}\right) - \tau\left(\chi + x_s + \frac{L}{2}\right) \right. \\ &\quad \left. + \tau\left(\chi - x_s - \frac{L}{2}\right) - \tau\left(\chi - x_s + \frac{L}{2}\right) \right]. \end{aligned} \quad (18)$$

With the aid of (14), (15), (17) and (18), the infinite double integral of (12) can be transformed into a finite one-dimensional integral as follows

$$\begin{aligned} I_{mn}^c &= \frac{1}{8} \int_{-L-x_s}^{2L-x_s} A(\chi) \tau\left(\chi + x_s - \frac{L}{2}\right) \chi d\chi \\ &\quad - \frac{1}{8} \int_{-2L-x_s}^{L-x_s} A(\chi) \tau\left(\chi + x_s + \frac{L}{2}\right) \chi d\chi \\ &\quad + \frac{1}{8} \int_{-L+x_s}^{2L+x_s} A(\chi) \tau\left(\chi - x_s - \frac{L}{2}\right) \chi d\chi \\ &\quad - \frac{1}{8} \int_{-2L+x_s}^{L+x_s} A(\chi) \tau\left(\chi - x_s + \frac{L}{2}\right) \chi d\chi \end{aligned} \quad (19)$$

The integral of (19) contains an integrable singularity. After the singular parts of integral are extracted analytically, the remaining nonsingular integration can be evaluated using a numerical procedure because the integral varies smoothly. This smooth behavior allows us to evaluate the numerical integration more accurately and timely.

4. EVALUATION OF THE INTEGRAL I_{mn}^c

Now we examine the finite one-dimensional integral of (19). The function $A(\chi)$ of one-dimensional integrals in (19) is a well-behaved function except for the singularity region. Within the interval of integration, the integral in (19) has an integrable singularity $\chi = 0$. The behavior of $A(\chi)$ can be approximated at and near the singularity $\chi = 0$ by

$$\begin{aligned} A^{Asy}(\chi) &= \lim_{\chi \rightarrow 0} A(\chi) \\ &= \left(\frac{2}{\pi}\right)^2 \left(\frac{2}{W}\right) \left[\frac{1}{2} \ln(16) - \frac{1}{2} \ln\left(2 \frac{|\chi|}{W}\right)\right]^2 \end{aligned} \quad (20)$$

Since the functions $A(\chi)$ and $\mathfrak{S}_c(\chi)$ are piecewise continuous, and the integration regions are determined by x_s , we need to consider three cases for evaluating the integrals in (19), which include $0 \leq x_s < L$, $L \leq x_s < 2L$, and $x_s \geq 2L$.

A. $0 \leq x_s < L$

In this case, there exists one singularity point within the integration regions $[-L-x_s, 2L-x_s]$, $[-2L-x_s, L-x_s]$, $[-L+x_s, 2L+x_s]$, and $[-2L+x_s, L+x_s]$ at $\chi = 0$, arising from $A(\chi)$. Thus, we subdivide the interval of integration into the three regions to the first integral in (19): one region at and near the singularity ($[-\Delta\chi, \Delta\chi]$) and two regions away from the singularity regions ($[-L-x_s, -\Delta\chi]$) and ($[\Delta\chi, 2L+x_s]$). The other three integrals in (19) can be subdivided with the same method. Away from the singularity regions, a numerical integration is used because the two functions $A(\chi)$ and $\mathfrak{S}_c(\chi)$ are well-behaved and vary slowly. Next, at and near the singularity regions, $A(\chi)$, $\tau(\chi+x_s-\frac{L}{2})$, $\tau(\chi+x_s+\frac{L}{2})$, $\tau(\chi-x_s+\frac{L}{2})$, and $\tau(\chi-x_s-\frac{L}{2})$ are approximated by their respective asymptotic function, and then the integrations are performed analytically. These lead to integrals of the form

$$\begin{aligned} & \int_{-L-x_s}^{2L-x_s} A(\chi) \cdot \tau\left(\chi+x_s-\frac{L}{2}\right) \chi d\chi \\ &= \int_{-L-x_s}^{-\Delta\chi} A(\chi) \cdot \tau\left(\chi+x_s-\frac{L}{2}\right) \chi d\chi \\ &+ \int_{-\Delta\chi}^{\Delta\chi} A^{Asy}(\chi) \cdot \tau^{Asy}\left(\chi+x_s-\frac{L}{2}\right) \chi d\chi \\ &+ \int_{\Delta\chi}^{2L-x_s} A(\chi) \cdot \tau\left(\chi+x_s-\frac{L}{2}\right) \chi d\chi \end{aligned} \quad (21)$$

If $A^{Asy}(\chi)$ and the original functions $\tau(\chi+x_s-\frac{L}{2})$ are used to evaluate the second integral of (21), a closed-form solution is possible. But it has an obviously complicated and lengthy form. Therefore, at and near the singularity region of $A(\chi)$, $\tau(\chi+x_s-\frac{L}{2})$ can also be approximated as a linear function at the local region of interest. In particular, we are interested in the interval $[x_s-\Delta\chi, x_s+\Delta\chi]$. In this region, $\tau^{Asy}(\chi+x_s-\frac{L}{2})$ is defined as

$$\tau^{Asy}\left(\chi+x_s-\frac{L}{2}\right) = \lim_{\chi \rightarrow 0} \tau\left(\chi+x_s-\frac{L}{2}\right) = a_0 \cdot \chi + \tau\left(\chi+x_s-\frac{L}{2}\right) \quad (22)$$

where $a_0 = \tau'\left(\chi+x_s-\frac{L}{2}\right)$ with respect to χ evaluated at $\chi = 0$.

Using (20) and (22), the second integral of (21) can be evaluated in closed-form as follows:

$$\begin{aligned}
 & \int_{-\Delta\chi}^{\Delta\chi} A^{Asy}(\chi) \cdot \tau^{Asy} \left(\chi + x_s - \frac{L}{2} \right) \chi d\chi \\
 &= \left(\frac{1}{\pi} \right)^2 \left[\frac{(\Delta\chi)^2}{W} \right] \tau \left(x_s - \frac{L}{2} \right) \left[1 + 12 \ln(2) \ln(W) + 6 \ln(2) \right. \\
 &\quad \left. + 2 \ln(W) + 18 \ln^2(2) + 2 \ln^2(W) - 12 \ln(2) \ln(\Delta\chi) - 2 \ln(\Delta\chi) \right. \\
 &\quad \left. + 2 \ln^2(\Delta\chi) - 4 \ln(\Delta\chi) \ln(W) \right] \quad (23)
 \end{aligned}$$

The function $a_0 \cdot \chi$ in (22) does not affect the results of the integral due to its odd property. Other three integrals in (19) can be performed with the same method.

B. $L < x_s < 2L$

In this case, there exists one singularity point in the integration regions $[-L - x_s, 2L - x_s]$ and $[-2L + x_s, L + x_s]$ at $\chi = 0$, arising from $A(\chi)$. The integral procedure is the same as the previous case. $A(\chi)$ does not have a singularity in the integration regions $[-2L - x_s, L - x_s]$ and $[-L + x_s, 2L + x_s]$. The integrals of (19) in the regions $[-2L - x_s, L - x_s]$ and $[-L + x_s, 2L + x_s]$ can be evaluated numerically using their respective functional representations of (19).

C. $x_s \geq 2L$

In the case of $x_s > 2L$, $A(\chi)$ does not have a singularity in the integration regions. Each integrand of (19) has a zero value as x_s approaches $2L$. Hence, the integrals in the regions can be evaluated numerically using their respective functional representations of (19).

The analytical integration at and near the singularity region is performed after replacing the original functions $A(\chi)$ and $\mathfrak{S}_c(\chi)$ by their respective asymptotic forms defined in (20) and (22); otherwise the numerical integration is carried out by using the self-adaptive integration scheme with the original functions $A(\chi)$ and $\mathfrak{S}_c(\chi)$. Using the three cases of A, B and C, we can now completely evaluate the finite one-dimensional integral in (19).

5. COMPUTATIONS AND COMPARISONS

The computing results of the original functions $A(\chi)$, $\tau(\chi + x_s - \frac{L}{2})$ for $W = L = 1$ mm when $x_s = 0, L/2$ have been given in Fig. 2. Also $A^{Asy}(\chi)$ is compared with its asymptotic function defined in (20). As

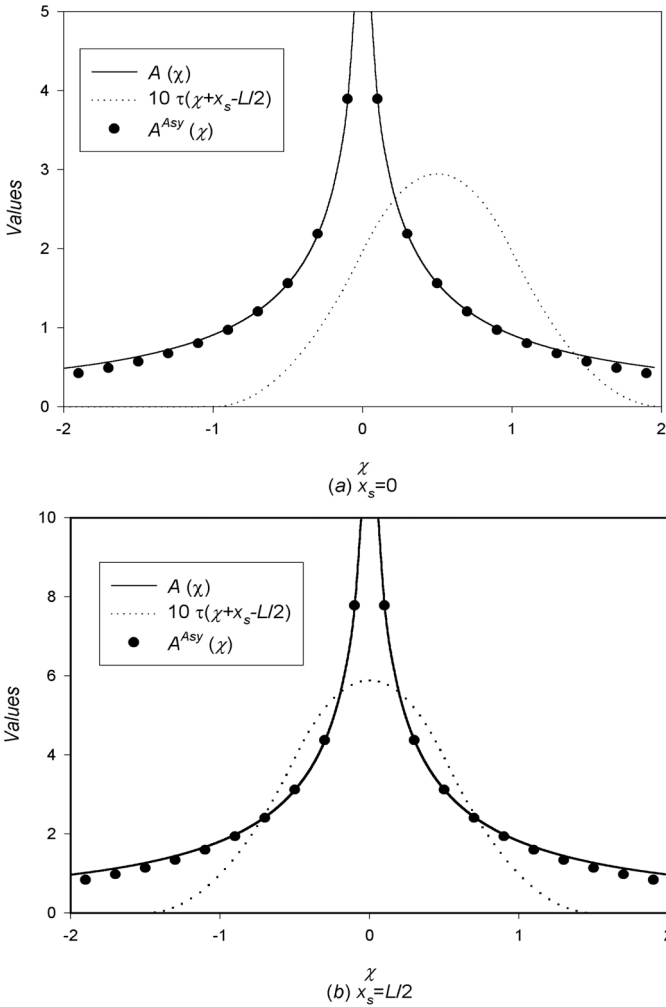


Figure 2. The values of $A(\chi)$, $A^{Asy}(\chi)$, and $10 \cdot \tau(\chi + x_s - \frac{L}{2})$ at $W = L = 1$ mm.

can be seen in Fig. 2, the original function $A(\chi)$ is well approximated by the asymptotic function defined in (20) at and near the singularity region.

To verify the proposed method, the result that obtained by the finite one-dimensional integration (19) was compared with the other by applying double infinite integration (12) and an upper limit $\beta^u = 400$ rad/mm. These results evaluated for $W = 0.60$ mm and

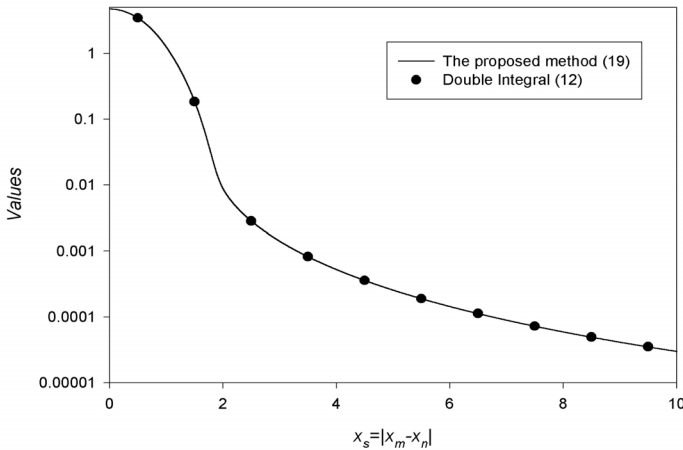


Figure 3. Comparison between the infinite two-dimensional integral and the finite one-dimensional method.

$L = 3.33$ mm, and different values of x_s from $0 \leq x_s \leq 10$ are plotted in Fig. 3, which indicate excellent agreement. In this paper, the proposed method can also be applied to evaluate the asymptotic part of impedance matrix, and dramatically reduce the computation time with improving the accuracy over the conventional method similar to that in [7].

6. CONCLUSION

Using the integral transform technique, the infinite double integral in the evaluation of the asymptotic part of the impedance matrix with triangular subdomain basis functions with edge condition was reduced to a finite one-dimensional integral for the analysis microstrip dipole on a uniaxial substrate. This finite one-dimensional integral can be easily evaluated numerically after the singular part of the integral is treated analytically. This finite one-dimensional integral significantly reduces the CPU time over the double integral. It is demonstrated the efficiency and accuracy of the proposed method to evaluate the asymptotic part of impedance matrix.

REFERENCES

1. Katéhi, P. B. and N. G. Alexópoulos, “Real axis integration of sommerfeld integrals with application to printed circuit antennas,”

- J. Math. Phys.*, Vol. 24, 527–533, 1983.
2. Mosig, J. R. and T. K. Sarkar, “Comparison of quasi-static and exact electromagnetic fields from a horizontal electric dipole above a lossy dielectric backed by an imperfect ground,” *IEEE Trans. Microwave Theory Tech.*, Vol. MTT-34, 379–387, 1986.
 3. Jackson, D. R. and N. G. Alexopoulos, “An asymptotic extraction technique for evaluating sommerfeld-type integrals,” *IEEE Trans. Antennas Propagat.*, Vol. AP-34, 1467–1470, Dec. 1986.
 4. Barkeshli, S., P. H. Pathak, and M. Martin, “An asymptotic closed-form microstrip surface Green’s function for the efficient moment method analysis of mutual coupling in microstrip antennas,” *IEEE Trans. Antennas Propagat.*, Vol. AP-38, 1374–1383, Sept. 1990.
 5. Chow, Y. L., J. J. Yang, D. H. Fang, and G. E. Howard, “Closed-form spatial green’s function for the thick substrate,” *IEEE Trans. Microwave Theory Tech.*, Vol. MTT-39, 588–592, Mar. 1991.
 6. Aksun, M. I. and R. Mittra, “Derivation of closed-form Green’s functions for a general microstrip geometry,” *IEEE Trans. Microwave Theory Tech.*, Vol. MTT-40, 2055–2062, Nov. 1992.
 7. Park, S. O. and C. A. Balanis, “Analytical techniques to evaluate the asymptotic part of the impedance matrix of Sommerfeld-type integrals,” *IEEE Trans. Antennas Propagat.*, Vol. 45, 798–805, 1997.
 8. Pozar, D. M., “Input impedance and mutual coupling of rectangular microstrip antennas,” *IEEE Trans. Antennas Propagat.*, Vol. AP-30, 1191–1196, Nov. 1982.
 9. Pozar, D. M., “Radiation and scattering from a microstrip patch on a uniaxial substrate,” *IEEE Trans. Antennas Propagat.*, Vol. AP-35, 613–621, June 1987.
 10. Pozar, D. M., “Improved computational efficiency for the method of moments solution of printed dipoles and patch,” *Electromagnetics*, Vol. 3, 299–309, 1983.
 11. Tan, J. and S. O. Park, “Comparison on the computation times for evaluating the impedance matrix elements in [12],” *A private Communication*, Apr. 1996.
 12. Pan, G. W. G., J. Tan, and J. D. Murphy, “Full-wave analysis of microstrip floating-line discontinuities,” *IEEE Trans. Electromag. Compatib.*, Vol. 36, 49–59, Feb. 1994.
 13. Jansen, R. H., “A modified least-squares boundary residual (LSBR) method and its application to the problem of shielded microstrip dispersion,” *Arch. Elek. Übertrag.*, Vol. 28, 275–277,

- 1974.
14. Schmidt, L.-P. and T. Itoh, "Characteristics of a generalized fin-line for millimeter wave integrated circuits," *International J. Infrared Millimeter Waves*, Vol. 2, 427–430, May 1981.
 15. Meixner, J., "The behavior of electromagnetic field at edges," *IEEE Trans. Antennas Propagat.*, Vol. AP-20, 442–446, July 1972.
 16. Gradshteyn, I. S. and I. M. Ryzhik, *Table of Integrals, Series, and Products*, Academic Press, New York, 1980.
 17. Abramowitz, M. and I. A. Stegun, *Handbook of Mathematical Functions*, Dover Publications, New York, 1972.
 18. Arabi, T. R., A. T. Murphy, T. K. Sarkar, R. F. Harrington, and A. R. Djordjević, "Analysis of arbitrarily oriented microstrip lines utilizing a quasi-dynamic approach," *IEEE Trans. Microwave Theory Tech.*, Vol. MTT-39, 75–82, Jan. 1991.
 19. Marin, M., S. Barkeshli, and P. H. Pathak, "Efficient analysis of planar microstrip geometries using a closed-form asymptotic representation of the grounded dielectric slab green's function," *IEEE Trans. Microwave Theory Tech.*, Vol. MTT-37, 669–679, Apr. 1989.